

Melting of Forsterite, Mg_2SiO_4 , From 9.7 to 16.5 GPaDEAN C. PRESNALL AND MICHAEL J. WALTER¹*Geosciences Program, University of Texas at Dallas, Richardson*

A multianvil apparatus has been used to determine the pressure-temperature melting curve of forsterite from 9.7 to 16.5 GPa. At 10.1 GPa a singular point occurs that marks the change from congruent melting at lower pressures to incongruent melting (forsterite = periclase + liquid) at higher pressures. The melting curve also passes through two invariant points. At one (15.6 GPa, 2310°C), the phases forsterite, periclase, anhydrous B, and liquid coexist and the melting reaction changes from forsterite = periclase + liquid at lower pressures to forsterite = anhydrous B + liquid at higher pressures. At the other (16.7 GPa, 2315°C), the phases forsterite, modified spinel, anhydrous B, and liquid coexist, and the melting reaction changes from forsterite = anhydrous B + liquid at lower pressures to modified spinel = anhydrous B + liquid at higher pressures. The Simon equation, $P(\text{GPa}) = 2.44[(T(^{\circ}\text{K})/2171)^{11.4} - 1]$, fits both our melting curve data and the lower pressure data of Davis and England (1964). At low pressures, the melting curve of forsterite lies at higher temperatures than that of enstatite, but the two curves cross at 13.3 GPa because of the lower dT/dP slope of the forsterite melting curve. This causes the forsterite-enstatite eutectic to shift toward forsterite as pressure increases, but our data are consistent with earlier findings that the shift is not sufficient to support an origin for the mantle by eutectic-like melting at high pressures.

INTRODUCTION

An understanding of the melting relationships of mantle materials at very high pressures is necessary in order to constrain models for the early melting and crystallization history of the Earth [e.g., Scarfe and Takahashi, 1986; Agee and Walker, 1988]. An initial step is the determination of the melting behavior of the major mantle minerals. Of these minerals, olivine is the most important. In this paper, we present data on the melting of forsterite, Mg_2SiO_4 , at pressures from 9.7 to 16.5 GPa. We also discuss the main features of the melting behavior of high-pressure polymorphs of forsterite up to 25 GPa and implications for the melting behavior of the mantle.

PREVIOUS WORK

Bowen and Andersen [1914] determined the melting temperature of forsterite at atmospheric pressure to be $1890 \pm 20^{\circ}\text{C}$ on the Geophysical Laboratory temperature scale [Sosman, 1952]. Conversion to the International Practical Temperature Scale of 1968 (IPTS-68) [Metrologia, 1969] used in this study gives a temperature of 1898°C . Davis and England [1964] used a piston-cylinder apparatus to determine the melting curve up to 5 GPa and fit a linear equation, $T(^{\circ}\text{C}) = 4.77P(\text{kbar}) + 1898$, to their data, which becomes $T = 4.77P + 1891$ when adjusted to IPTS-68. The difference between their extrapolated 1-atm melting point of 1891°C and the melting point determined by Bowen and Andersen is within experimental uncertainty.

More recent studies using multianvil presses have extended the melting relationships to much higher pressures. Ohtani and Kumazawa [1981] showed congruent melting behavior up to the limit of their study at 15 GPa but expressed confidence in this type of melting only up to a pressure of 12.7 GPa. Kato

and Kumazawa [1985a, 1986] reported that forsterite melts incongruently to periclase + liquid at 15 GPa, $2220 \pm 40^{\circ}\text{C}$. At 20 GPa, they reported that Mg_2SiO_4 (modified spinel) melts incongruently to phase B + liquid at $2250 \pm 20^{\circ}\text{C}$ and that phase B then melts incongruently to periclase + liquid at the slightly higher temperature of $2280 \pm 20^{\circ}\text{C}$. Using a multianvil apparatus, Kato and Kumazawa [1985b] determined the melting temperature of forsterite to be $1975 \pm 35^{\circ}\text{C}$ at 3 GPa and $2125 \pm 20^{\circ}\text{C}$ at 7 GPa. Their temperature at 3 GPa is lower than the earlier value of 2034°C (adjusted to IPTS-68) determined by Davis and England [1964] with a piston-cylinder apparatus. Also, the melting temperature found by Kato and Kumazawa [1985a] at 15 GPa is about 250°C lower than that indicated by Ohtani and Kumazawa [1981]. In order to resolve these differences and to determine the pressure stability ranges for the incongruent melting reactions found by Kato and Kumazawa, we have studied the melting of forsterite from 9.7 to 16.5 GPa with runs closely spaced in pressure.

EXPERIMENTAL PROCEDURE

Experiments were performed with the split-sphere multianvil apparatus (UHP-2000) at the University of Alberta, Canada. The experimental procedures are identical to those described by Presnall and Gasparik [1990] except that the octahedrons used were made of 95% MgO, 5% Cr_2O_3 instead of pure MgO. All experiments were done with an octahedron of 10-mm edge length, WC cubes with 5-mm truncations, a W3Re/W25Re thermocouple positioned axially within a cylindrical LaCrO₃ heater, and a Re sample capsule. Temperatures were not corrected for the effect of pressure on thermocouple emf. To remove water, the octahedron assembly, including the sample capsule, was fired in argon for 1 hour at 1000°C immediately prior to each experiment.

The pressure calibration is tied directly to that used by Presnall and Gasparik [1990] at State University of New York at Stony Brook. They located the clinoenstatite-majorite transition at 16.5 GPa, 2150°C , relative to the pressure calibration described by Gasparik [1989] and found that this transition is nearly independent of temperature, as expressed

¹Now at Geophysical Laboratory, Carnegie Institution of Washington, Washington, D. C.

Copyright 1993 by the American Geophysical Union.

Paper number 93JB01007.
0148-0227/93/93JB-01007\$05.00

by the equation, $P(\text{GPa}) = 17.36 - 0.0004T(^{\circ}\text{C})$. Thus it is an excellent transition to use as a pressure calibration at high temperature. The pressure cell assembly at the University of Alberta was calibrated against this transition at 2050°C. Three experiments, each 1 hour in duration, were performed at 0.2-GPa intervals, with pure MgSiO_3 prepared by firing an oxide mixture twice at 1650°C with intermediate grinding. At the lowest pressure, the charge consisted entirely of clinoenstatite; at the highest pressure, it consisted entirely of majorite; and at the intermediate pressure, the phase boundary was found within the capsule, with clinoenstatite being located in the cold end. The consistency of these three experiments suggests that the pressure uncertainty is less than ± 0.2 GPa.

A second calibration point is the coesite-stishovite transition. Quartz powder was used as a starting material and runs were held at temperature for 6 hours. In the defining experiment, the coesite-stishovite transition was found toward the cool part of the capsule at a temperature of about 1150°C. At this temperature, the data of *Yagi and Akimoto* [1976] indicate a pressure for the transition of 9.3 GPa. The resulting pressure calibration curve is shown in Figure 1.

The starting composition for all the experiments was a powder of Mg_2SiO_4 composition prepared by T. Gasparik and generously supplied to us. He had taken the ground oxide mixture through two cycles of firing (1300°C for 24 hours) and regrinding. To be sure no traces of other phases remained, we fired (1600°C) and reground the powder four additional times. The first of these firings lasted 1 hour and the other three lasted 2 hours each. Microscopic examination of the final powder in oil revealed no phases other than forsterite.

As in the study of *Presnall and Gasparik* [1990], the sample capsule was positioned with the hot spot slightly displaced from the center of the capsule toward the thermocouple tip. Temperatures of phase boundaries in longitudinal polished sections of the capsules were then determined on the basis of

the isotherms shown in Figure 2 of *Presnall and Gasparik* [1990]. Temperature uncertainty of these phase boundaries is estimated to be $\pm 30^{\circ}\text{C}$.

The liquid region of a recovered sample always consisted entirely of forsterite quench crystals in a matrix that was found by microprobe analysis to have the composition of MgSiO_3 . The feathery texture of the forsterite quench crystals allowed them to be distinguished easily from equilibrium crystals in other parts of the capsule. Electron microprobe analyses were performed on the JEOL 8600 instrument at The University of Texas at Dallas. Olivine was distinguished from modified spinel by brightness differences in backscattered electron images and by differences in fluorescence colors produced by the electron beam (olivine, dim purple; modified spinel, bright green).

TIME-TEXTURE RELATIONSHIPS IN EXPERIMENTAL RUN PRODUCTS

We have found a strong effect of time on the textural development of run products that is a potential source of confusion in the determination of melting relationships. The changes with time are the combined effect of a thermal gradient, diffusion in the liquid, and small but unavoidable temperature fluctuations. For a liquid coexisting with crystals in a thermal gradient, *Lesher and Walker* [1988] distinguished two driving forces for diffusion in the liquid. One of these, the Soret effect, results from the existence of a temperature gradient and causes diffusion leading to compositional variations in an initially homogeneous liquid. The second, which they referred to as saturation gradient chemical diffusion, results from variations with temperature in the solubility of minerals in the melt.

Figures 2 and 3 are backscattered electron images of two run products that show the textural changes produced by different run times. The run shown in Figure 2 was held at temperature for 3 min. Here, quench crystals of clinoenstatite (? , light gray) and forsterite (dark gray) in the hot part of the capsule are separated from forsterite in the cold part by a band that consists partly of periclase (black) + quench crystals and partly of periclase + forsterite. Figure 3 shows a sample held at the same pressure and nearly the same temperature for 43 min. Here, the phase assemblages from the hot to the cold parts of the capsule change progressively and symmetrically from quench crystals to a band of forsterite, then to a band of forsterite + periclase (dominated by periclase), and finally to an area of forsterite. The symmetrical distribution pattern of crystals about the hot zone of the capsule demonstrates that gravitational crystal settling did not occur.

In order to address the cause of the textural changes between Figures 2 and 3, it is necessary to determine which driving force for diffusion identified by *Lesher and Walker* [1988] is operative. As a test for the existence of Soret diffusion, we examined experiment 403 (Figure 3) for compositional differences between the hottest and coldest parts of the quenched liquid. To minimize the difficulty of obtaining a bulk analysis of the fine intergrowth of enstatite (?) and forsterite quench crystals, the electron beam was enlarged to 5 μm . Even with this precaution, large variations in composition were obtained, so averages were taken of the compositions of a large number of 5- μm spots. In Figure 3 the hot area analyzed lies near the right-hand wall of the capsule about midway between the upper and lower bands of equilibrium crystals. The cold area analyzed is a curved band at a roughly constant

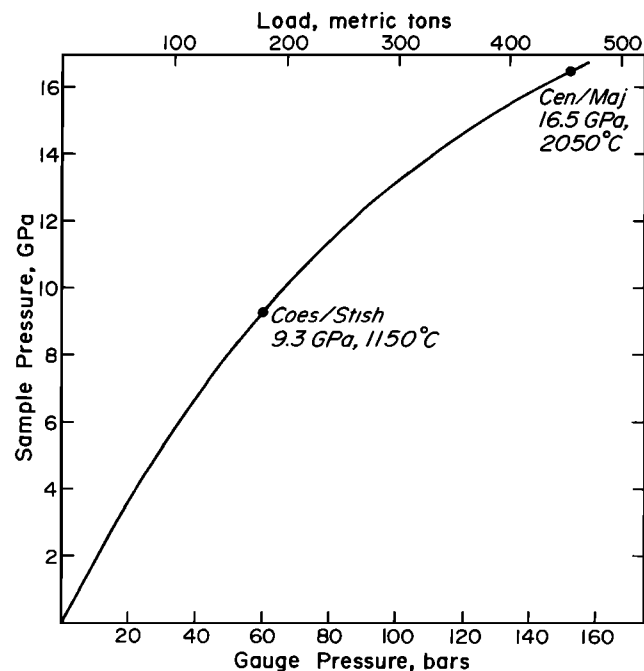


Fig. 1. Pressure calibration curve at high temperatures for octahedron assembly with a 10-mm edge length and an anvil truncation of 5 mm. The coesite-stishovite transition is from *Yagi and Akimoto* [1976] and the clinoenstatite-majorite transition is from *Presnall and Gasparik* [1990].

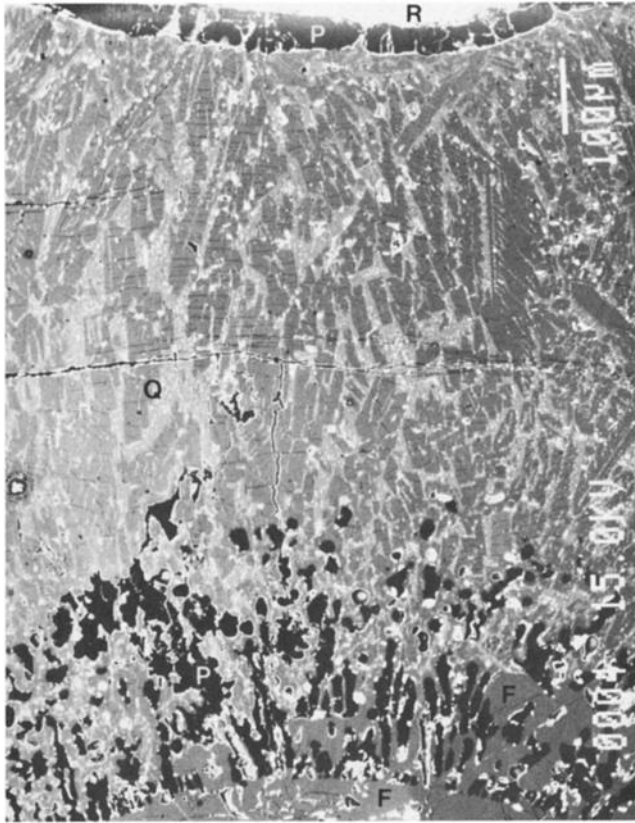


Fig. 2. Backscattered electron image of experiment at 14 GPa, 2310°C (nominal temperature) for 3 min (run 393, Table 1). The section is a longitudinal cut through the center of the cylindrical capsule with the thermocouple located just above the top of the image, which is also the top of the capsule as it rested in the apparatus. R, rhenium capsule, F, forsterite; P, periclaise; Q, quench crystals. The hottest part of the capsule is about 350 μm from the top of the photograph. Only the hotter upper half of the capsule is shown. Note boundary near the bottom of the photograph that separates a band of forsterite + spinel (above) from pure unmelted forsterite (below).

distance of about 40 μm from the lower boundary of the quench crystal region. The temperature difference between these two areas is estimated to be about 40°C. Averages of 29 spots in the hot area and 29 spots in the cold area gave SiO_2 concentrations (normalized to a $\text{SiO}_2 + \text{MgO}$ sum of 100%) of $50.9 \pm 1.1\%$ (standard deviation of the mean) and $50.2 \pm 1.1\%$, respectively. These concentrations are statistically identical, so no measurable Soret effect exists. No elements other than Mg and Si were detected.

In the absence of a significant amount of Soret diffusion, the textural differences between Figures 2 and 3 must be explained by saturation gradient chemical diffusion. We do this with the aid of a schematic phase diagram (Figure 4). First, we consider the result of suddenly placing a sample of uniform bulk composition, A, into a temperature gradient that does not change with time. On the assumption of instantaneous attainment of equilibrium, the initial sequence of phase assemblages along a traverse from the hot to the cold part of the capsule would be liquid, periclaise + liquid, and forsterite; and the initial composition of the liquid would change gradually from composition A at the hot margin of the periclaise + liquid zone to composition B at the cold margin. With time, diffusion would eliminate the compositional gradient and produce a uniform liquid composition somewhere between A and B. This

is the process that *Leshner and Walker* [1988] called saturation gradient chemical diffusion. Figure 4 shows, however, that a liquid of uniform composition would be unstable and that periclaise would dissolve at the hot margin and crystallize at the cold margin. The net result would be to thin the periclaise + liquid zone, expel liquid from it, and enrich it in periclaise.

In the top part of Figure 2 a nearly monomineralic zone of periclaise is already developed after only 3 min. In Figure 3 the layers strongly enriched in periclaise are well developed after 43 min and the lower of these layers is narrower and more enriched in periclaise than the lower periclaise + liquid zone in Figure 2, exactly as expected.

Now we consider the effects of small temperature fluctuations that would always be present in any experiment. Prior to complete development of the periclaise-rich layer and homogenization of the liquid composition, as in Figure 2, the coolest part of the liquid would have a composition close to B. A downward temperature fluctuation at this time would move this coolest part of the liquid into the forsterite + liquid field, and forsterite would crystallize between the surrounding periclaise crystals. Thus the periclaise-rich layer would not be monomineralic but would contain some interstitial forsterite, as is observed in both experiments. Figure 3b shows that channels occupied by forsterite extend completely through the periclaise-rich layer. Thus, even after mature development of the periclaise-rich layer and homogenization of the liquid composition, the textural relationships show that forsterite and periclaise both would remain in contact with liquid. Figure 4 shows that the composition of the liquid at this stage would lie at B. Also, the temperature of the interface between liquid and the periclaise-rich layer would be T_p because at equilibrium, forsterite, periclaise, and liquid would all be in contact with each other along an isotherm in the capsule. If the temperature controller were then to allow temperatures throughout the capsule to decrease quickly, a new layer of forsterite + liquid would form between the periclaise-rich layer and the liquid. With time, it would compact by saturation gradient chemical diffusion to a monomineralic layer as in Figure 3.

On the other hand, if the temperature controller were to allow the temperature to increase, the interface between liquid and the periclaise-rich layer would be eroded by melting and the reaction, forsterite = periclaise + liquid, would proceed to the right. Thus forsterite would dissolve at the interface and periclaise would crystallize. This would thin the periclaise-rich layer and replace part of it by a new layer of periclaise + liquid. If the temperature then were to stabilize, the new periclaise + liquid layer would thin and become enriched in periclaise as explained above. However, a continuing increase in temperature would cause further erosion of the periclaise-rich layer as well as dissolution of periclaise in the newly formed periclaise + liquid layer. Thus, although increasing temperature can cause crystallization of phases (in this case, periclaise), upward temperature fluctuations tend to destroy crystalline textures produced at earlier stages of the experiment. Thermal erosion of this type appears to exist in the lower left portion of Figure 2. During all of these changes, the direction of diffusion in the liquid will be generally perpendicular to isotherms in the charge. The elongate shape of many of the periclaise crystals perpendicular to isotherms (Figures 2 and 3) is consistent with this type of mass flux in the liquid that surrounds them. *Leshner and Walker* [1988] also noted this feature.

These considerations underscore the difficulties and potential risks in determining crystal-liquid phase relationships from

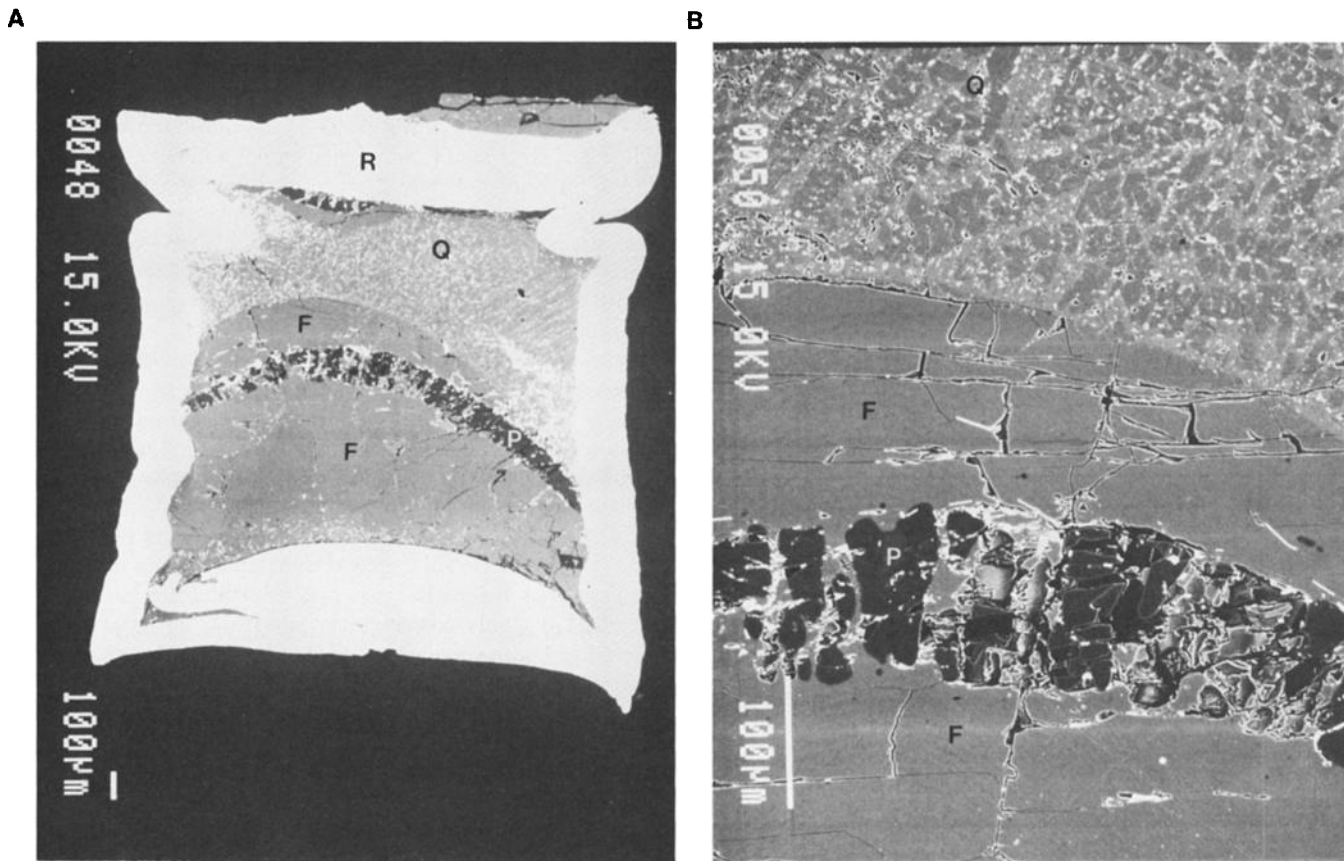


Fig. 3. Backscattered electron image of experiment at 14 GPa, 2270°C (nominal temperature) for 43 min (run 403, Table 1) at (a) low and (b) high magnification. Orientation and labels are the same as in Figure 2.

experiments on samples held in a strong temperature gradient. For the simple binary phase relationships encountered in this study, the effects of the temperature gradient can be understood. However, for a multicomponent system with many different reactions taking place across the temperature gradient, the danger of misinterpretation is increased. A procedure that some have used [e.g., *Herzberg et al.*, 1990] is to note the crystal-liquid phase assemblages that occur as temperature decreases across the capsule. On the assumption that the bulk composition of the sample remains constant throughout the capsule, this procedure yields complete information about the phase relationships from the liquidus to the solidus. However,

as we have shown, the validity of this assumption degrades rapidly as the run duration increases. Even for a run duration of 3 min, significant departures from spatial homogeneity of the sample can occur (Figure 2).

Thus a dilemma occurs. If run durations are held to very short times (1 or 2 min, at most, for our experiments), progressively changing phase assemblages across a temperature gradient may be reasonably assumed to be relevant to the bulk composition of the sample powder placed in the capsule. However, chemical equilibrium cannot be assured for such short experiments. On the other hand, if run durations are extended in order to assure equilibrium, then the phase assemblages observed are prone to misinterpretation. The only totally satisfactory solution to the dilemma would be to eliminate temperature gradients across the sample and make runs long enough that equilibrium could be assured. Caution in interpreting the results of melting experiments should increase in proportion to the extent that experimental conditions deviate from this ideal.

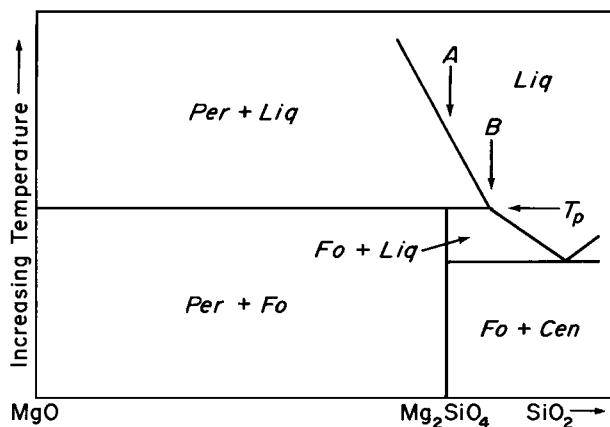


Fig. 4. Schematic phase diagram to explain textural development of run products. Liq, liquid; Cen, clinoenstatite; Per, periclase; Fo, forsterite.

MELTING CURVE OF FORSTERITE

Figure 5 shows the melting curve of forsterite up to 16.5 GPa, and Table 1 lists the experiments on which this curve is based. The experiment in Table 1 at 16.5 GPa is taken from *Presnall and Gasparik* [1990] and was done by T. Gasparik at State University of New York at Stony Brook using the same pressure calibration as that used here. The melting temperature determined from this experiment is consistent with melting temperatures determined from 9.6 to 14.9 GPa (Table 1) at the University of Alberta. The data in Figure 2 lie along a smooth

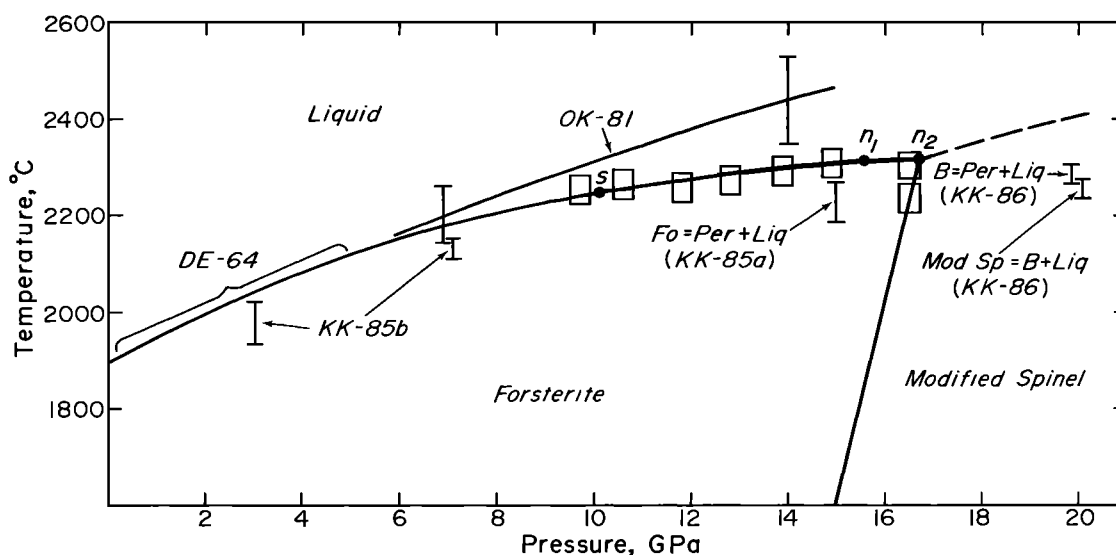


Fig. 5. Melting curve of forsterite, Mg_2SiO_4 . Rectangular boxes are runs reported in Table 1 except for the box on the forsterite/modified spinel transition at 2230°C, 16.5 GPa, which is from *Presnall and Gasparik* [1990, Table 1]. Size of boxes represents experimental uncertainty of $\pm 30^\circ C$ and ± 0.2 GPa. Data points represent temperatures of phase boundaries within capsules, not nominal run temperatures. Solid circles show locations of singular (s) and invariant (n_1 and n_2) points. Comparisons with other data are as follows: OK-81, *Ohtani and Kumazawa* [1981]; DE-64, *Davis and England* [1964]; KK-85a, *Kato and Kumazawa* [1985a]; KK-85b, *Kato and Kumazawa* [1985b]; KK-86, *Kato and Kumazawa* [1986]. Brackets at 7 and 20 GPa are separated slightly in pressure to avoid confusion from overlapping lines. Anhb, anhydrous B [$Mg_{14}Si_5O_{24}$]; B, phase B [$Mg_{12}Si_4O_{19}(OH)_2$]; Mod Sp, modified spinel [Mg_2SiO_4]. Other abbreviations are as in Figure 4. Note that the reaction Mod Sp = B + Liq is not balanced because Mod Sp is anhydrous. This reaction simply expresses the phases observed by *Kato and Kumazawa* [1986]. Position of dashed curve is inferred.

extension of the lower pressure data of *Davis and England* [1964]. Although *Davis and England* fit a straight line to their data, the slightly curved line shown in Figure 5 is an equally good fit and is required by the higher pressure data reported here.

In Figure 5, the singular point (s) at 10.1 GPa, 2250°C, marks the change from congruent melting of forsterite at lower pressures to incongruent melting (forsterite = periclase + liquid) at higher pressures. *Schreinemakers* [1916] has shown that no discontinuity in the slope of a melting curve occurs at a singular point even though the melting reaction changes at this point. Therefore, the melting curve has been shown without a break in slope as it passes through s. The pressure of

10.1 GPa for the singular point is a correction to our value reported earlier of 10.5 GPa [*Presnall and Walter*, 1989]. This earlier value was based on an error in the pressure calibration curve.

At about 15.6 GPa, 2310°C, an invariant point (n_1) occurs that corresponds to the equilibrium assemblage forsterite + periclase + anhydrous B + liquid. Anhydrous B has the composition $Mg_{14}Si_5O_{24}$ and its structure was determined by *Finger et al.* [1989] on a crystal extracted from the experiment at 16.5 GPa listed in Table 1. At the invariant point, the incongruent melting reaction of Mg_2SiO_4 changes from forsterite = periclase + liquid at lower pressures to forsterite = anhydrous B + liquid at higher pressures. In contrast to the situation for the singular point discussed above, invariant point n_1 causes a discontinuity in the T-P slope of the forsterite melting curve to produce a slightly lower slope at higher pressures. This difference in slope cannot be resolved experimentally but is required by *Schreinemakers'* rules [*Zen*, 1966].

A second invariant point (n_2) is shown at 16.7 GPa, 2315°C, at which the phases forsterite, modified spinel, anhydrous B, and liquid are in equilibrium. At n_2 , the incongruent melting reaction of Mg_2SiO_4 changes from forsterite = anhydrous B + liquid at lower pressures to modified spinel = anhydrous B + liquid at higher pressures. Although an upper pressure bracket for this invariant point has not been determined along the forsterite melting curve, the pressure is well constrained by the forsterite/modified spinel transition. The straight line for this transition shown in Figure 5 passes through the point at 16.5 GPa, 2230°C determined by *Presnall and Gasparik* [1990], through the point at 15.0 GPa, 1600°C reported by *Katsura and Ito* [1989], and between the experiments of *Katsura and Ito* that show forsterite at 13.9 GPa, 1200°C, and modified spinel at 14.4 GPa, 1200°C. This consistency suggests close agreement

TABLE 1. Experiments on the Composition Mg_2SiO_4

Run	P, GPa	T, °C		Time, min
		Nominal	Boundary ^a	
492	9.7	2210	2250(C)	5
410	10.6	2220	2260(P)	14
408	11.8	2240	2255(P)	18
405	12.8	2260	2270(P)	10
393 ^b	13.9	2310	2275(P)	3
403	13.9	2270	2290(P)	43
402	14.9	2280	2305(P)	7
^c	16.5	2380	2300(A) ^d	120

^aAbbreviations for phase boundaries: C, congruent melting temperature, no periclase; P, forsterite/(periclase + liquid) peritectic; A, forsterite/(anhydrous B + liquid) peritectic.

^bRun not shown on Figure 5.

^cExperiment on forsterite reported in *Presnall and Gasparik* [1990, Table 1].

^dThis temperature is corrected from the temperature of 2350°C given by *Presnall and Gasparik* [1990, Table 1].

between the pressure calibration used here and that used by *Katsura and Ito* [1989]. The dP/dT slope of this line, $0.0024 \text{ GPa}/^\circ\text{C}$, is nearly identical to but slightly less than that given by *Suito* [1977] and at the upper uncertainty limit of that calculated by *Akaogi et al.* [1989]. It is also essentially identical to the slope of $0.00236 \text{ GPa}/^\circ\text{C}$ given by equation (2) of *Gasparik* [1990].

We have fitted a single Simon equation to all of our data on the melting of forsterite up to 14.9 GPa and the lower pressure data of *Davis and England* [1964]. The equation is

$$P = 2.44 \left[\left(\frac{T}{2171} \right)^{11.4} - 1 \right]$$

where temperature T is in degrees kelvin, and pressure P is in gigapascals. The constant, 2171, is the melting temperature of forsterite at atmospheric pressure. The use of a single Simon equation for the melting curve above and below the singular point s might be considered improper because the curve involves two different reactions. This problem could be addressed by fitting two different equations, one to the data below 10.1 GPa, and another to the data above. However, this would produce a slight discontinuity in slope where the two curves meet, a situation in violation of the topological constraint that no discontinuity in slope exists at a singular point [*Schreinemakers*, 1916]. Thus we avoid the problem of a discontinuity by using a single expression and treat the Simon equation as simply an empirical representation of our results.

In Figure 5 the forsterite melting curve determined in this study is compared with previous determinations. The melting curve of *Ohtani and Kumazawa* [1981] lies at temperatures as much as 150°C higher than the melting curve we have determined. Also, *Ohtani and Kumazawa* reported congruent melting behavior up to at least 12.7 GPa, whereas we find that incongruent melting begins at about 10.1 GPa. Although these discrepancies appear to be large, they are not. At 7 GPa the temperature uncertainty bracket given by *Ohtani and Kumazawa* overlaps our curve, and at 15 GPa the lower limit of their temperature uncertainty bracket is only slightly above

our curve (Figure 5). Our data are in disagreement with only one experiment of *Ohtani and Kumazawa*, a run that yielded unmelted forsterite at 12.7 GPa, $2360 \pm 30^\circ\text{C}$ (their Table 1, run 80102).

The melting temperatures of *Kato and Kumazawa* [1985a, b, 1986], who used a multianvil apparatus, are systematically lower than those of other studies at all pressures (Figure 5). Of particular significance is their melting temperature of $1975 \pm 35^\circ\text{C}$ at 3 GPa. This is about 60°C lower than the value reported by *Davis and England* [1964]. Because temperature gradients and pressure uncertainties are smaller in the piston-cylinder apparatus used by *Davis and England*, their temperature is preferred to that of *Kato and Kumazawa*. Our data lie along a smooth extension of the data of *Davis and England*.

Kato and Kumazawa [1985a] reported that at 15 GPa, forsterite melts incongruently to periclase and liquid (Figure 5). They also reported [*Kato and Kumazawa*, 1986] that at 20 GPa, modified spinel melts incongruently to phase B + liquid and that phase B then melts incongruently to periclase and liquid. If the temperature differences between our results and those of *Kato and Kumazawa* [1985a, 1986] are ignored and if phase B reported by them is actually anhydrous B (see discussions by *Herzberg and Gasparik* [1989] and *Presnall and Gasparik* [1990, p. 15,774]) our result are consistent with their data.

Figure 6 shows a pressure-temperature isopleth for Mg_2SiO_4 based on the present work and other studies at higher pressures. Two additional invariant points, n_3 and n_4 , are shown. The subsolidus univariant lines for the reactions, modified spinel = spinel, perovskite + periclase = spinel, and modified spinel = perovskite + periclase, are after *Gasparik* [1990]. Invariant point n_4 (modified spinel + perovskite + periclase + liquid) is placed at 2650°C , 22.6 GPa, based on the data of *Gasparik* [1990]. The location of invariant point n_3 (periclase + modified spinel + anhydrous B + liquid) has not been determined, but it must lie at a pressure less than that of n_4 . If the phase that *Kato and Kumazawa* [1986] called B (see Figure 5) is actually anhydrous B, then n_3 must also lie at a pressure greater than 20 GPa. It has been placed at 21 GPa, 2420°C .

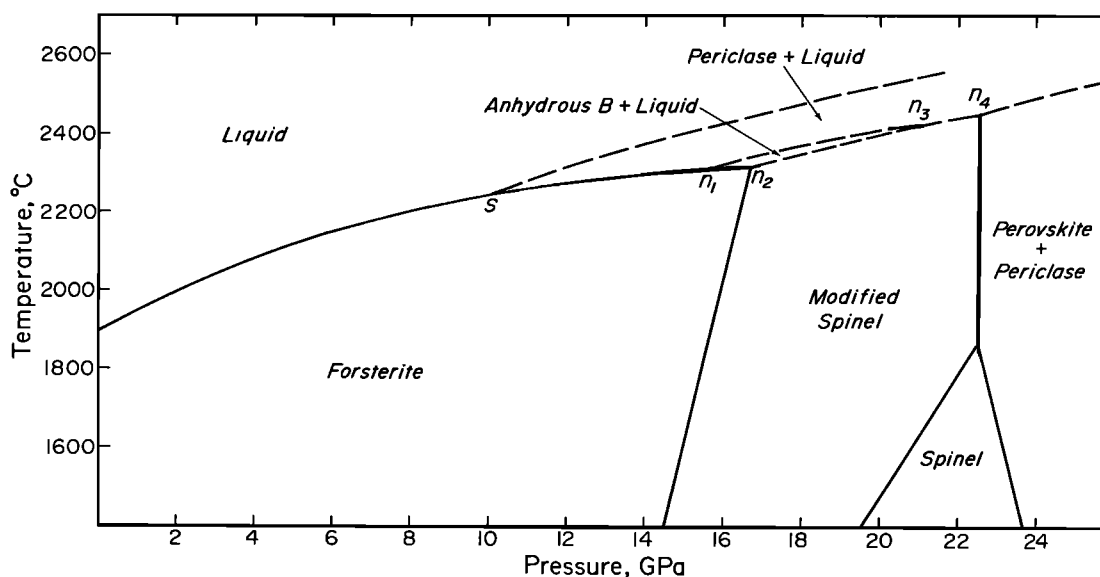


Fig. 6. Temperature-pressure isopleth for the composition Mg_2SiO_4 . Subsolidus phase boundaries at pressures above 20 GPa are from *Gasparik* [1990]. Positions of dashed curves are inferred. All phase boundaries are univariant curves except the dashed curve separating the liquid field from the periclase + liquid field.

IMPLICATIONS FOR MELTING OF THE MANTLE

The dT/dP slope of the enstatite melting curve [Presnall and Gasparik, 1990] is much greater than that of forsterite. As a result, the two curves cross at 13.3 GPa, and the melting temperature of enstatite is about 20°C higher than that of forsterite at 16.5 GPa. These differences in slope form part of the basis for the suggestion that the eutectic between forsterite and enstatite shifts strongly toward forsterite with pressure and that the composition of upper mantle peridotite is controlled by eutectic-like melting at about 16 GPa [Herzberg and O'Hara, 1985; Takahashi, 1986]. However, Presnall and Gasparik [1990] pointed out that although increasing pressure does cause the eutectic to shift toward forsterite, the shift is too small to support the concept of eutectic-like melting for the origin of mantle peridotite at about 16 GPa. Our results are consistent with the conclusions of Presnall and Gasparik. Herzberg et al. [1990] have also rejected the eutectic-like melting model.

At pressures above 22.6 GPa, modified spinel is not stable at solidus temperatures (Figure 6), so the melting behavior of model lherzolite would be governed by the eutectic between periclase and perovskite. If further work shows that the composition of this eutectic decreases in SiO₂ with increasing pressure, the eutectic-like melting model for the origin of the mantle might be revived, but the process would take place at a pressure much greater than that originally proposed. If the shift is toward SiO₂ with pressure, eutectic-like melting would be an unlikely origin for the mantle at any pressure.

Acknowledgments. We thank T. Gasparik for providing some of the ceramic parts used in the pressure cell assemblies and for the forsterite powder used as a starting material. We thank C. Herzberg and, especially, D. Walker for helpful journal reviews. The experiments were done with the split-sphere multianvil apparatus at the University of Alberta, supported by NSERC Infrastructure grant CII0006947. Presnall thanks the geology faculty at the University of Alberta for this and other financial support and for their very gracious hospitality. This work was also supported by National Science Foundation grants EAR-8418685 and EAR-8816044 and by Texas Advanced Research Program grants 3927, 009741-007, and 009741-066. Geosciences Program, University of Texas at Dallas, contribution 752.

REFERENCES

- Agee, C. B., and D. Walker, Mass balance and phase density constraints on early differentiation of chondritic mantle, *Earth Planet. Sci. Lett.*, **90**, 144-156, 1988.
- Akaogi, M., E. Ito, and A. Navrotsky, Olivine-modified spinel-spinel transitions in the system Mg₂SiO₄-Fe₂SiO₄: Calorimetric measurements, thermochemical calculation, and geophysical application, *J. Geophys. Res.*, **94**, 15,671-15,685, 1989.
- Bowen, N. L., and O. Andersen, The binary system MgO-SiO₂, *Am. J. Sci.*, **37**, 487-500, 1914.
- Davis, B. T. C., and J. L. England, The melting of forsterite up to 50 kilobars, *J. Geophys. Res.*, **69**, 1113-1116, 1964.
- Finger, L. W., J. Ko, R. M. Hazen, T. Gasparik, R. J. Hemley, C. T. Prewitt, and D. J. Weidner, Crystal chemistry of phase B and an anhydrous analogue: Implications for water storage in the upper mantle, *Nature*, **341**, 140-142, 1989.
- Gasparik, T., Transformation of enstatite-diopside-jadeite pyroxenes to garnet, *Contrib. Mineral. Petrol.*, **102**, 389-405, 1989.
- Gasparik, T., Phase relations in the transition zone, *J. Geophys. Res.*, **95**, 15,751-15,769, 1990.
- Herzberg, C. T., and M. J. O'Hara, Origin of mantle peridotite and komatiite by partial melting, *Geophys. Res. Lett.*, **12**, 541-544, 1985.
- Herzberg, C. T., and T. Gasparik, Melting experiments on chondrite at high pressures: Stability of anhydrous phase B, *Eos Trans. AGU*, **70**, 484, 1989.
- Herzberg, C. T., T. Gasparik, and H. Sawamoto, Origin of mantle peridotite: Constraints from melting experiments to 16.5 GPa, *J. Geophys. Res.*, **95**, 15,779-15,803, 1990.
- Kato, T., and M. Kumazawa, Stability of phase B, a hydrous magnesium silicate, to 2300°C at 20 GPa, *Geophys. Res. Lett.*, **12**, 534-535, 1985a.
- Kato, T., and M. Kumazawa, Effect of high pressure on the melting relation in the system Mg₂SiO₄-MgSiO₃, I, Eutectic relation up to 7 GPa, *J. Phys. Earth*, **33**, 513-524, 1985b.
- Kato, T., and M. Kumazawa, Melting and phase relations in the system Mg₂SiO₄-MgSiO₃ at 20 GPa under hydrous conditions, *J. Geophys. Res.*, **91**, 9351-9355, 1986.
- Katsura, T., and E. Ito, The system Mg₂SiO₄-Fe₂SiO₄ at high pressures and temperatures: Precise determination of stabilities of olivine, modified spinel, and spinel, *J. Geophys. Res.*, **94**, 15,663-15,670, 1989.
- Leshner, C. E., and D. Walker, Cumulate maturation and melt migration in a temperature gradient, *J. Geophys. Res.*, **93**, 10,295-10,311, 1988.
- Metrologia*, The international practical temperature scale of 1968, **5**, 35-44, 1969.
- Ohtani, E., and M. Kumazawa, Melting of forsterite Mg₂SiO₄ up to 15 GPa, *Phys. Earth Planet. Inter.*, **27**, 32-38, 1981.
- Presnall, D. C., and T. Gasparik, Melting of enstatite (MgSiO₃) from 10 to 16.5 GPa and the forsterite (Mg₂SiO₄) - majorite (MgSiO₃) eutectic at 16.5 GPa: Implications for the origin of the mantle, *J. Geophys. Res.*, **95**, 15,771-15,777, 1990.
- Presnall, D.C., and M.J. Walter, Incongruent melting of Mg₂SiO₄ to periclase + liquid (10.5-16 GPa) and AnhB + liquid (>16 GPa), *Eos Trans. AGU*, **70**, 1419, 1989.
- Scarfe, C. M., and E. Takahashi, Melting of a garnet peridotite PHN-1611 to 13 GPa: Implications for the evolution of the upper mantle, *Nature*, **322**, 354-356, 1986.
- Schreinemakers, F. A. H., In-, mono-, and di-variant equilibria. VIII. Further consideration of the bivariate regions; the turning lines, *Proc. K. Akad. Wet. (Netherlands)*, **18**, 1539-1552, 1916.
- Sosman, R. B., Temperature scales and silicate research, *Am. J. Sci., Bowen Vol.*, 517-528, 1952.
- Suito, K., Phase relations of pure Mg₂SiO₄ up to 200 kilobars, in *High-Pressure Research: Applications in Geophysics*, edited by M. H. Manghnani and S. Akimoto, pp. 255-266, Academic Press, San Diego, Calif., 1977.
- Takahashi, E., Melting of a dry peridotite KLB-1 up to 14 GPa: Implications on the origin of peridotitic upper mantle, *J. Geophys. Res.*, **91**, 9367-9382, 1986.
- Yagi, T., and S. Akimoto, Direct determination of coesite-stishovite transition by in-situ X-ray measurements, *Tectonophysics*, **35**, 259-270, 1976.
- Zen, E., Construction of pressure-temperature diagrams for multicomponent systems after the method of Schreinemakers — A geometric approach, *U. S. Geol. Survey Bull.* **1225**, 56 pp, 1966.

D. C. Presnall, Geosciences Program, University of Texas at Dallas, P. O. Box 830688, Richardson, TX 75083-0688.

M. J. Walter, Geophysical Laboratory, Carnegie Institution of Washington, 1530 P Street, N. W. Washington, DC 20005.

(Received March 9, 1992;
revised April 5, 1993;
accepted April 14, 1993.)